Colloid Polym Sci (2007) 285:1201–1211
DOI 10.1007/s00396-007-1673-1

ORIGINAL CONTRIBUTION

Linear viscoelastic properties of electro-rheological nano-suspension confined to narrow gap between electrodes

Katsufumi Tanaka · Hyota Nakahori · Kazutaka Katayama · Ryuichi Akiyama

Received: 5 January 2007 / Accepted: 11 March 2007 / Published online: 30 March 2007

Abstract The linear viscoelastic properties of a suspension composed of titanium dioxide nanoparticles were measured under the direct current (dc) electric field with narrow gap distances between the electrodes. The yielding behavior under no external electric fields was also discussed. The wall slip at the interface between the parallel plates and the nano-suspension was briefly discussed. Under the dc electric field, a fine chain-like microstructure was optically found within a narrow gap of 50 μm between the electrodes in the quiescent state. The nano-suspension confined to a narrow gap of 65 μm between the parallel plates was rather viscoelastic even at the highest strength of the electric field of 16 kV· mm^{-1}. Furthermore, fast and slow relaxations of the dynamic moduli were found after removal of the electric field. It was pointed out that the linear viscoelasticity was an appropriate measure of the microstructure before yielding.

Keywords Electro-rheology · Nano-particles · Linear viscoelasticity · In situ optical observations · DC electric field

Introduction

The electro-rheological effect, in short, the ER effect, is the reversible rheological response of fluids only by the application and removal of an external electric field [1]. A suspension composed of microparticles and insulating oil shows the ER effect [2–5], and the micro-suspension is a typical ER fluid. In the micro-suspension, the primary particles are randomly distributed without external electric fields. When the electric field is applied, the particles are polarized and a chain-like microstructure along the electric field is induced. A columnar microstructure, which is further composed of electrically ordered chains of microparticles, is sometimes found between the electrodes. The microstructure is closely related to the ER effect of the micro-suspension.

For practical applications of the ER suspension, stability against sedimentation of the particles, and applicability to a narrow gap between the electrodes are required for micro- or nano-devices. Much larger yield stresses are also demanded, and the rheological properties should be evaluated with a narrow gap corresponding to such applications. Therefore, the nano-suspension is a promising ER fluid. At the same time, the ER effect with a narrow gap between the electrodes is of great interest. Recently, we reported the ER effect of a suspension composed of titanium dioxide (TiO_2) nanoparticles with the primary particle diameter of 15 nm [6]. The suspended particles were remarkably stable against sedimentation, and the nano-suspension showed a good fluidity under the steady shear flow with a gap of 50 μm.

It is worthwhile to note that the flow without external electric fields is not assumed to be the Newtonian flow, but the Bingham flow with an apparent yield stress, σ_{y0}. A microstructure in the nano-suspension would dynamically develop and disappear by the particle–particle interaction without external electric fields. At the same time, the nano-suspension was electrically stable. The apparent yield stress, $\sigma_y(E)$, of more than 3 kPa was induced by the dc electric field with a strength, E, of 16 kV· mm^{-1}. The ER effect was also induced by the sinusoidal electric field with frequencies up to 1 kHz.

K. Tanaka (✉) · H. Nakahori · K. Katayama · R. Akiyama
Department of Macromolecular Science and Engineering,
Graduate School of Science and Technology,
Kyoto Institute of Technology, Matsugasaki,
Kyoto 606-8585, Japan
e-mail: ktanaka@kit.ac.jp

Furthermore, a fine chain-like microstructure and a much smaller structure of aggregates within a single chain have been preliminarily found with our in situ optical observations under external electric fields in the quiescent state. The electrically induced chain-like microstructure would be responsible for the ER effect of the nano-suspension, which is apparently similar to the ER effect of the micro-suspension. However, it is important that the hierarchical structure of the nanoparticles has been found within a fine single chain. The chain is composed of aggregates which are further composed of primary and secondary particles. The ER effect of the nano-suspension will be clarified in detail by further rheological investigations.

Figure 1 shows a hypothetical stress–strain curve for slow deformations. The dashed line indicates hysteresis, which can occur before maximum. It is assumed that the static yield stress is not necessarily the same as the dynamic yield stress in the figure [7], while the definition of the yield stress may be unique for specific rheological models. Experimentally, the value or even the existence of a yield stress could depend on the duration of the experiment, and the meaning of the yield stress is not necessarily universal [7–9]. The dynamic yield stress would be measured in a constant shear rate experiment using a strain-controlled rheometer, while the static yield stress would be measured using a stress rheometer. Further, the stresses for the proportional limit and the elastic limit shown in Fig. 1 can be defined as the yield stress.

For a suspension having a microstructure of particles, the stress for the elastic limit may be practically the same as the static (or dynamic) yield stress because the yielding of the microstructure and the flow of the suspension would be induced beyond the elastic limit. Therefore, the dynamic yield stress under steady shear flow is a measure of the microstructure after yielding. On the other hand, the linear viscoelasticity is an appropriate measure of the microstructure before yielding, just like the chain-like microstructure observed in the quiescent state. The viscoelastic properties around the proportional limit (or the elastic limit) would be measured in this case. Furthermore, the rheological behavior of the microstructure having the hierarchical structure of nanoparticles within a single chain would essentially be viscoelastic.

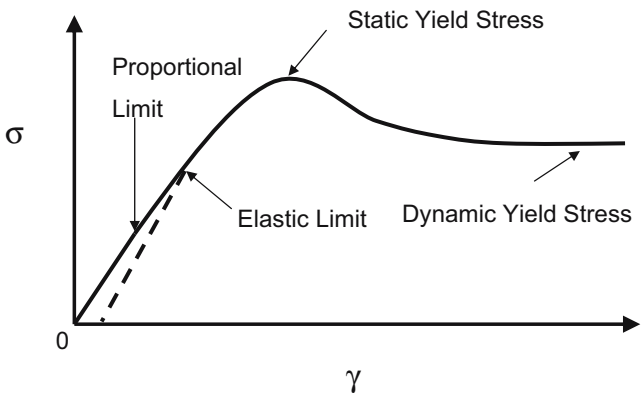

Fig. 1 A hypothetical stress–strain curve for slow deformations. The *dashed line* indicates hysteresis, which can occur before maximum

In the present paper, the linear viscoelastic properties are reported for a suspension composed of TiO_2 nanoparticles under the dc electric field with narrow gap distances between the electrodes. The yielding behavior under no external electric fields is also reported. The wall slip at the interface between the parallel plates and the nano-suspension is discussed briefly. To investigate the slippage [10], the dynamic measurements were performed with different gap distances between the parallel plates. If the microstructure is ideal and defect-free between the parallel plates, the yield stresses measured with different gap distances are identical in the case of a negligibly small wall slip.

On the other hand, it is practical to assume an imperfect microstructure in a real nano-suspension including a macroscopic defect such as the boundary of the aggregates (or microstructure). In this case, the defect would act as the weakest spot in the whole volume of the nano-suspension between the parallel plates (electrodes). The total number of the defect is proportional to the gap distance between the parallel plates assuming the homogeneous distribution of the defect in the whole volume and a constant area of the sample on the plates. Therefore, it is important to investigate the effect of the gap distance on the flow behavior. For practical applications, as mentioned previously, the flow behavior within a narrow gap is also important for micro- or nano-devices.

In-situ optical observations of the nano-suspension are also reported under the dc electric field. The dependence of the storage and loss moduli on the electric field strength is discussed in relation to the microstructure found under the dc electric field. Furthermore, responses and relaxations of the dynamic moduli induced by application and removal of the stepwise electric field are also reported.

Experimental

Rutile TiO_2 nanoparticles with the nominal average diameter of the primary particles of 15 nm (MT-150A, TAYCA Corporation) were suspended in a silicone oil with the viscosity of 5×10^{-2} Pa·s and the dielectric constant of 2.7. (From the electron microscopic observation by the supplier, the shape and the surface of the primary particles are reported to be slightly elongated and mostly smooth, respectively. The number averaged diameter of the particles was determined to be 18 nm with the standard deviation of 10 nm. The mode of the particle diameters was 15 nm.) The volume fraction of the particles was 8.8×10^{-2} [6].

Both the nanoparticles and the silicone oil were sufficiently dried in a vacuum oven before the sample preparation. Therefore, the residual water is sufficiently reduced in both the particles and silicone oil. The nanoparticles were manually milled in an agate mortar with a pestle before they were dried. The dried particles were mixed with the silicone oil by the use of a magnetic stirrer for several hours. The rotational speed of a stirring bar was not indicated numerically, but adjusted to a little intense level of rotation on a full scale of approximately 1,200 rpm.

As pointed out below, the conduction current was sufficiently lower than the noise level even under the electric field of 16 kV·mm^{-1}. Furthermore, no electrophoresis was found during our in situ optical observations under the dc electric field. Therefore, the nanoparticles and the silicone oil are well assumed to be dielectrics in the present study.

The viscoelastic measurement with a small oscillatory shear strain was performed at room temperature using a strain-controlled rotational rheometer (Rheology Co., MR-300V2E) and fixtures of parallel plates. (Before the viscoelastic measurement of the nano-suspension, a silicone oil with the viscosity of 5×10^2 Pa·s was measured with a gap of 65 μm and a diameter of 18 mm, and the resultant dynamic viscosity at lower angular frequencies was in good agreement with the reported viscosity.) The dc electric field was also applied to the sample sandwiched between the parallel plates (electrodes). The diameter of the parallel plates was 24 mm for the measurements under no electric fields and the electric field with a strength of 0.1 kV·mm^{-1}. The gap distance between the plates was 300 or 500 μm. Above 0.5 kV·mm^{-1}, the diameter of the parallel plates was 10 mm. The gap distance between the plates was 100 or 200 μm for 0.5 and 1 kV·mm^{-1}; and 65 or 100 μm above 2 kV·mm^{-1}. At each electric field strength, the strain amplitude was carefully set so that the linear response of stress to strain was well assumed.

Before each viscoelastic measurement, the nano-suspension was pre-sheared at a constant shear rate of 200 s^{-1} for 30 s, and kept in the quiescent state for 300 s. Subsequently, the sinusoidal strain with an angular frequency of ω and an amplitude of γ_0 was applied. Typically, the sinusoidal response is obtained for the stress with an amplitude of σ_0 and the phase difference between the strain and stress, δ, in the case of the linear response. (During the viscoelastic measurement, the conduction current passing through the nano-suspension was monitored in a similar way as reported elsewhere [11], but the conduction current was sufficiently lower than the noise level).

With our rheometer, the waveforms of the stress and strain can be recorded at the same time. In case of the non-linear response, the fundamental component of the stress wave with an amplitude of σ_1 was extracted from the distorted wave, and the dynamic moduli of $G_1^{'}$ and $G_1^{''}$ were calculated using the following equations:

$$G_1^{'}=(\sigma_1/\gamma_0)\cos\delta_1 \quad (1)$$

$$G_1^{''}=(\sigma_1/\gamma_0)\sin\delta_1, \quad (2)$$

where δ_1 is the phase difference between the strain wave and the extracted stress wave. For the calculation of γ_0, a small rotational displacement of the upper plate, which is attached to the torque sensor, was corrected [12, 13]. In this study, the phase difference of δ_1 (or δ) was also determined using the waveforms of the corrected strain and stress by digital Fourier transformation.

Particle behavior was observed using an optical microscope (Nikon, Eclipse E600W) equipped with a CCD camera. A small amount of the nano-suspension was placed between the electrodes of tin-doped indium oxides (ITO) with a gap of approximately 50 μm. The image data were recorded with a VTR and transferred to a PC [14].

Results and discussion

Linear viscoelastic properties and yielding behavior under no external electric fields

Figure 2a,b show the angular frequency dependence of the storage moduli, a, and the loss moduli, b, of the nano-suspension measured under no external electric fields with different gap distances and various preset amplitudes of the oscillatory strain. The storage (or loss) moduli measured at a preset amplitude with different gap distances mostly coincide in the figure, except for the moduli measured at the lower frequencies of strain. The difference between the moduli can be caused by the weak responses of torque at the lower frequencies, and wall slip was not remarkable for the TiO_2 nano-suspension under no external electric fields.

The storage and loss moduli are independent of the preset strain amplitude below 0.75%. At the larger strain amplitudes, both the storage and loss moduli at a given angular frequency decrease with an increase in the amplitude of the strain in the figure. Correspondingly, the Lissajous figures were distorted. Therefore, the linear viscoelastic properties were measured with preset strain amplitudes of 0.4 and 0.5%. Further, G' and G'' are mostly independent of ω. Therefore, it is solid-like before yielding even under no external electric fields.

It is of great interest that the nano-suspension is partly elastic with the non-zero value of G', which is intrinsically different from the ER micro-suspension. Under no electric fields, G' is essentially zero for the micro-suspension because the flow of the micro-suspension is Newtonian in

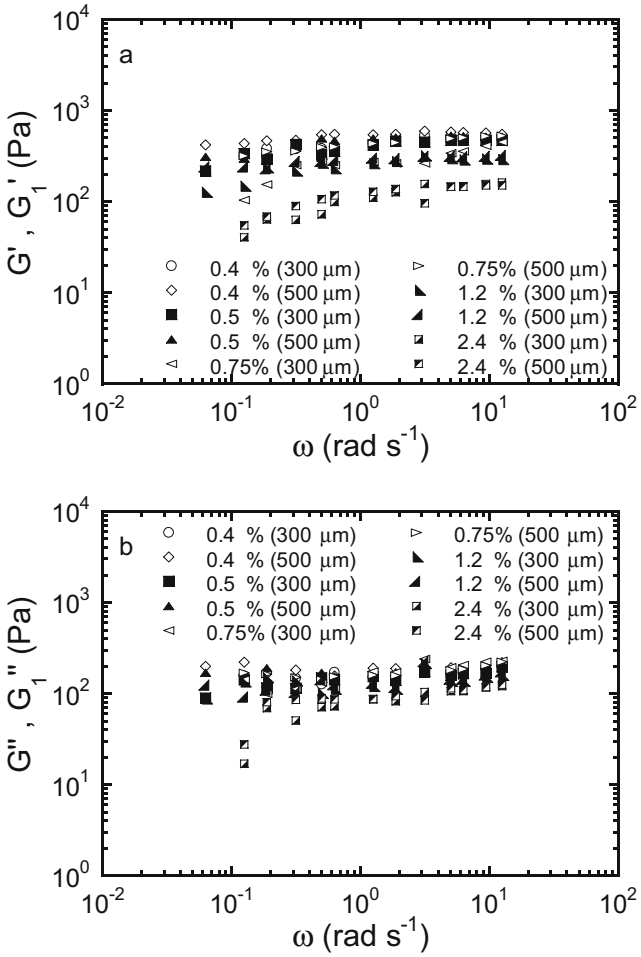

Fig. 2 The angular frequency dependence of the storage moduli (**a**) and the loss moduli (**b**) of the nano-suspension measured at various preset amplitudes of the oscillatory strain under no external electric fields. The gap distance between the parallel plates was 300 or 500 μm

terms of both theory and experiment [5, 15]. For an ER suspension with sub-micrometer particles of monodispersed silica with the weight-averaged diameter of 0.45 μm and a volume fraction of 0.4 [16], a slightly pseudoplastic flow at low shear rates was reported under no electric fields. However, the suspension showed no elastic responses in the dynamic measurement without electric fields.

In the nano-suspension, a microstructure with a long-term relaxation would be developed by the particle–particle interaction without external electric fields. At the same time, each nanoparticle in the nano-suspension would join in and leave from the microstructure locally and dynamically on a time scale much shorter than ω^{-1}, because the thermal fluctuation of the Brownian motion was not negligible during our in situ optical observations. However, it is not easy to clarify the microstructure under no external electric fields by direct observations. Therefore, the viscoelastic measurement is effective for discussing the microstructure in further detail.

From the viscoelastic parameters shown in Fig. 2a and b, σ_1 at an angular frequency was calculated using Eqs. (1) and (2). The linear response of σ_0 was calculated similarly. Figure 3 shows σ_0 and σ_1 plotted logarithmically against the corrected strain amplitude, γ_0, measured at ω of 1.9 rad· s^{-1}. In the figure, tanδ and tanδ_1 are also plotted. The stress amplitude of σ_0 is proportional to γ_0 up to 0.5%, while tanδ shows smaller values. At γ_0 of 1.2 and 2.4%, σ_1 increases only a little, while tanδ_1 shows larger values. (As discussed in Experimental, σ_1 is the fundamental component of the distorted stress wave with the higher order harmonics, and it is only a part of the total stress response.) At γ_0 of 0.75%, the stress amplitude and loss tangent measured with a gap of 300 μm show smaller and larger values, respectively, which may be related to the wall slip at the strain amplitude.

Therefore, a microstructure developed under no external electric fields would yield to the strain. The yield strain is estimated to be around 0.75%, and the corresponding stress to be 3.4 Pa. At the largest γ_0, σ_1 may be closely related to the dynamic yield stress, which is measured under steady shear flow. However, the stress amplitude σ_1 was 4 Pa and the peak stress, σ_p, calculated from the distorted torque wave was 5 Pa at most. Apparently, these stresses measured under oscillatory shear deformation are somewhat smaller than the apparent yield stress σ_{y0} of 10 Pa measured with a gap of 50 μm under steady shear flow at a shear rate of 1.9 s^{-1} [6]. There are two possible reasons for the difference, other than wall slip and experimental error.

In Fig. 3, the yielding for the proportional limit would be measured because G' and G'' were independent of strain smaller than 0.75%. Therefore, the estimated stress amplitude of 3.4 Pa would be the stress for the proportional limit and slightly smaller than the dynamic yield stress as shown in Fig. 1.

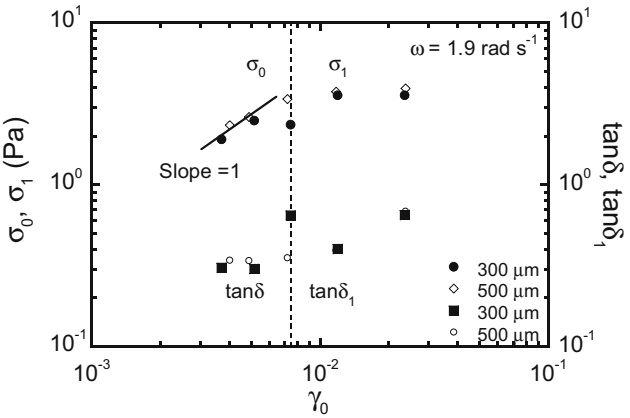

Fig. 3 The stress amplitudes of σ_0 and σ_1 plotted logarithmically against the strain amplitude, γ_0 with ω of 1.9 rad· s^{-1}. In the figure, tanδ and tanδ_1 are also plotted. The stress amplitudes were calculated using the viscoelastic parameters shown in Fig. 2a and b. The strain amplitude was corrected in the figure

Another possible reason is the difference in the gap and the diameter of the parallel plates between the two measurements; both the gap and the diameter used in the dynamic measurement under no electric fields, 300 or 500 μm in gap and 24 mm in diameter, are much larger than those used in the steady shear measurement, 50 μm in gap and 18 mm in diameter. In our preliminary measurement under steady shear flow with a gap and diameter of 500 μm and 40 mm, respectively, the apparent yield stress was about 5 Pa, which agrees well with σ_1 (or σ_p). The stress measured with the narrower gap was slightly larger than that with the wider gap. It is somewhat difficult to explain the tendency due to wall slip; the effect of wall slip can be remarkable for a narrow gap compared to a wide gap, and the critical stress for wall slip is smaller than the dynamic (or static) yield stress for the bulk of a nano-suspension.

In the real nano-suspension, the primary particles usually form secondary particles or much larger aggregates, and further form a microstructure such as a three-dimensional network. If the microstructure is ideal and defect-free between the parallel plates, the yield stresses measured with different gap distances are identical in the case of a negligibly small wall slip. However, a macroscopic defect such as the boundary of the aggregates (or microstructure) would act as the weakest spot anywhere in the whole volume of the nano-suspension between the parallel plates when the gap is wide enough. Then, the smaller yield stress is measured for the parallel plates with a wider gap distance. The increase in the diameter of the plates would affect the yield stress similarly.

Under steady shear flow, the dynamic yield stress would be measured appropriately with a sufficiently narrow gap so that macroscopic defect was unable to develop within the gap. However, the difference in the measured stresses was relatively small for conclusion, and the narrower gap distance was limited to 300 μm in the dynamic measurement shown in Fig. 2 because of the weak torque responses in the linear region. Further study is needed to discuss the problem in detail.

In situ optical observations for nano-suspension under the dc electric field

In the present study, in-situ optical observations of our nano-suspension without any dilution were performed under the dc electric field in the quiescent state. Figure 4a shows a captured video image of the nano-suspension under no external electric fields. A significant microstructure, which would be responsible for the plateau-like behavior of G' shown in Fig. 2a, cannot be found with sufficient contrast under no external electric fields. At much higher electric field strengths than 2 kV·mm^{-1}, a fine chain-like microstructure was clearly seen along the electric field. As shown in Fig. 4b–e, a single chain spans the electrodes, and it develops more clearly as the strength of the electric field increases.

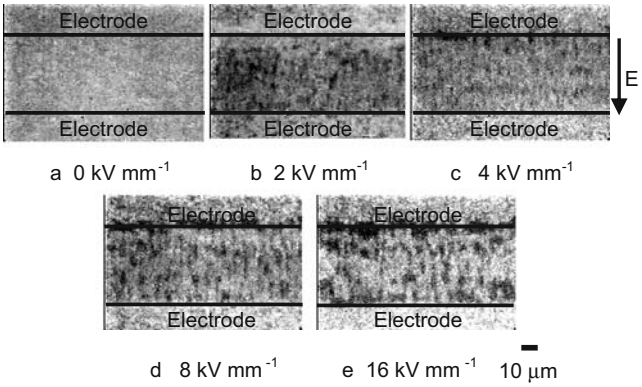

Fig. 4 Captured video images of the nano-suspension in the quiescent state under no external electric fields (**a**), at 2 kV·mm^{-1} (**b**), at 4 kV·mm^{-1}(**c**), at 8 kV·mm^{-1} (**d**), and at 16 kV·mm^{-1} (**e**)

At the higher electric field strengths, the chain-like microstructure would be more stable and defect-free along the electric field. (In addition, no electrophoresis was observed under the dc electric field.) Therefore, the chain-like microstructure induced by the external electric field is responsible for the ER effect of the nano-suspension, which is apparently similar to the ER effect of the micro-suspension. However, the width of a single chain was on the order of micrometers, and the chain developed within the narrow gap of 50 μm. Such a fine chain-like microstructure could not be composed of microparticles with a diameter on the order of 10 μm.

Further, it is of great interest that a single chain is hierarchically composed of nanoparticles; single chain is not homogeneous, but is composed of aggregates, which are further composed of primary and secondary particles. The storage modulus of the nano-suspension having such a microstructure of a single chain would increase with an increase in the strength of the electric field. In addition, thermal fluctuation of the Brownian motion was not negligible during our real-time observations. Therefore, the nano-suspension under the dc electric field would show a viscoelastic behavior rather than the purely elastic behavior, which is discussed in the next section.

Linear viscoelastic properties under the dc electric field

Figure 5a and b shows G' and G'', respectively, plotted logarithmically against ω. Typical examples of the Lissajous figure are shown in Fig. 6. The storage (or loss) moduli measured at an angular frequency and strength of the electric field with different gap distances above 2 kV·mm^{-1} mostly coincide in Fig. 5. Below 2 kV·mm^{-1}, slight

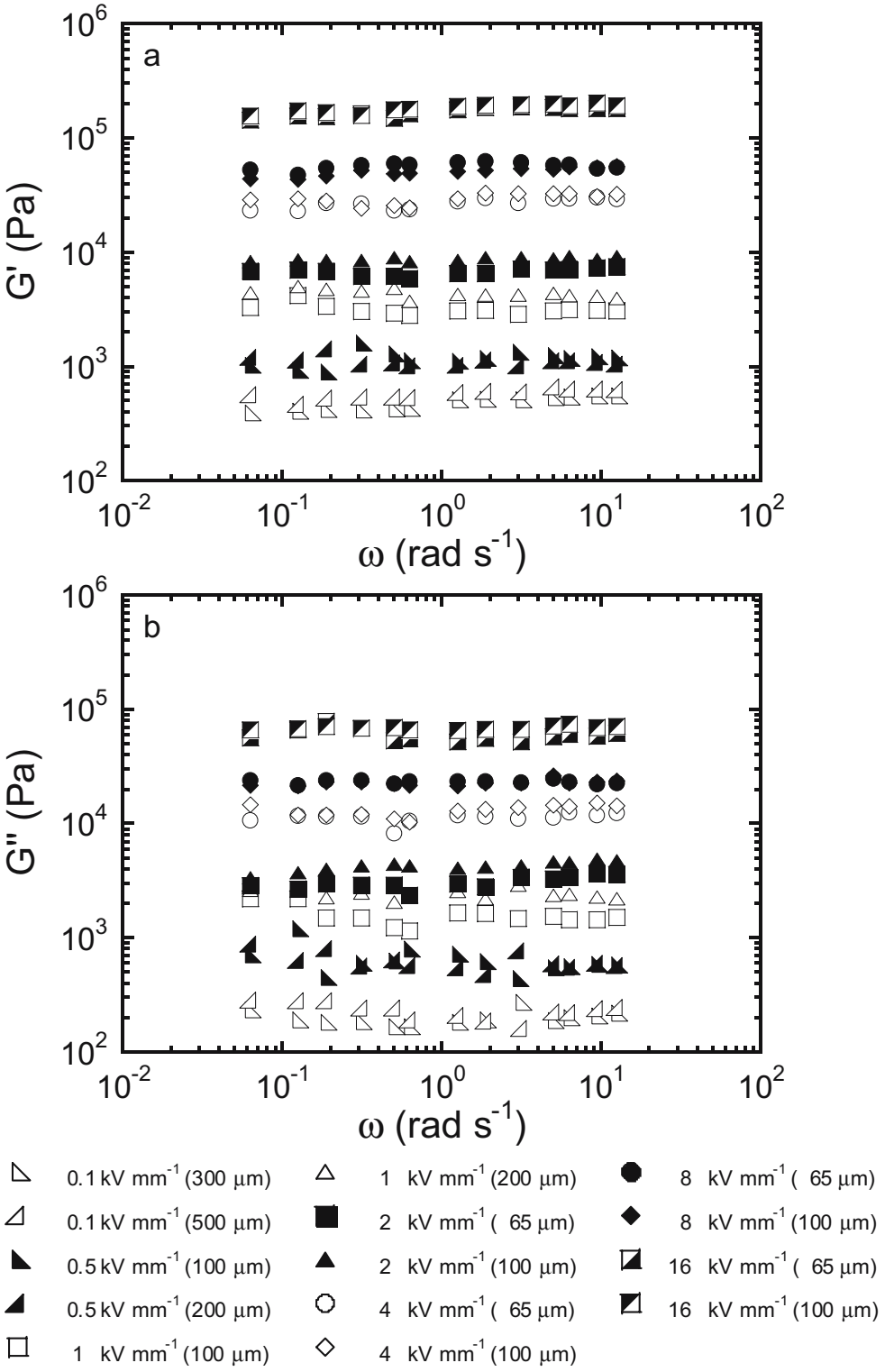

Fig. 5 The angular frequency dependence of the storage moduli (**a**) and the loss moduli (**b**) of the nano-suspension measured at different strengths of the dc electric field. The gap distance between the parallel plates was 65, 100, 200, 300, or 500 μm. For the linear response of the stress, the amplitude of the oscillatory strain was chosen depending on the strength of the electric field

differences are found between the storage (or loss) moduli measured with different gap distances. As previously reported, the steady shear stresses measured with different gap distances under the dc electric field above 1 kV·mm^{-1} were almost identical [6]. Similar to Fig. 2, the difference can be caused by weak responses of torque at the lower strengths of the electric field. It can also be thought that the nano-suspension was unstable, including some defects at strengths lower than 2 kV·mm^{-1}, partly because the gap distances were relatively wider and the strain amplitude for a linear response decreased as the strength of the electric field decreased.

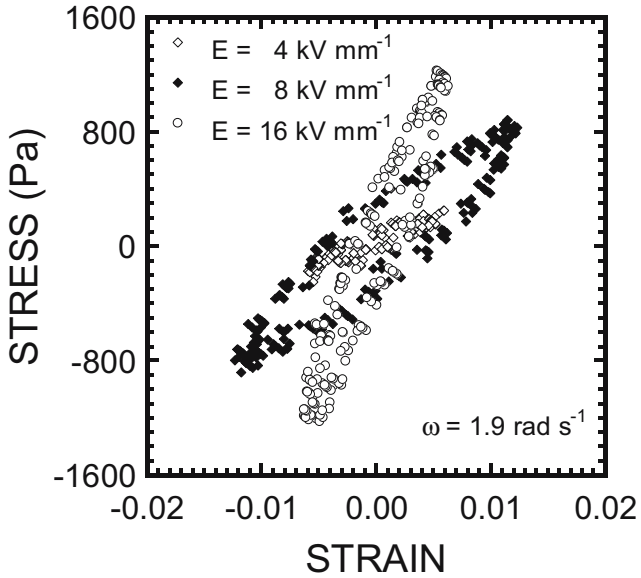

Fig. 6 Typical examples of Lissajous figure for the dynamic measurement with a gap of 65 μm and ω of 1.9 rad·s^{-1} shown in Fig. 5

In Fig. 5, G' (or G'') at a given electric field strength is mostly independent of ω, suggesting that the nano-suspension is solid-like before yielding. Similar plateaus shown in Fig. 5a and b were reported for the ER micro-suspension [5] measured using a stress-controlled rheometer with a small stress under the electric field. However, strong frequency dependences were reported for the ER micro-suspension with a little larger stress under the electric field. An appearance of plateaus was also observed with a stress slightly below the Bingham (dynamic) yield stress, which can be associated with the yielding of structure with an infinite relaxation time. For another ER micro-suspension [15], strong frequency dependences of the dynamic moduli were reported especially under weak electric fields.

Furthermore, the frequency dependence of the Maxwell-type relaxation was typically observed at very small strains under the electric field for the ER suspensions with sub-micrometer particles of monodispersed silica with volume fractions of 0.2 and 0.4 [16]. Beyond a critical strain, plateaus were also observed, showing the yielding of structure. Among these results, the viscoelastic responses associated with the yielding of structure would be nonlinear.

The frequency dependence of G'' also suggests that the nano-suspension under the dc electric field cannot be approximated by the Voigt model, although fully developed chains spanning the electrodes can be seen in Fig. 4. Further, it is of interest that the Lissajous figure measured at 16 kV·mm^{-1} is still elliptic, and the nano-suspension was rather viscoelastic.

As discussed above, typical examples of the Maxwell model with a single relaxation mode were reported for the ER suspensions with sub-micrometer particles [16]. The plastic response was also found for the ER micro-suspension in the creep measurement [5]. The energy dissipation for these ER suspensions was explained by the hydrodynamic interactions with drifting chains, and chains attached at only one end to an electrode [5, 16]. The shear-induced structural changes of the thick column from an ordered lattice [17] to another metastable configuration were proposed for the plastic response [5]. Furthermore, a significant and sharp relaxation was simulated for a thick cluster composed of a single-sphere-width strand with two additional strands placed along each side of the original strand [15]. The energy dissipation was discussed in terms of the hydrodynamic relaxation of the electrostatically driven sphere motion.

In our nano-suspension, both G' and G'' at a given strength of the electric field are mostly independent of ω, which cannot be approximated by the Maxwell model as well. However, the energy dissipation would be induced within each single chain-like microstructure of nanoparticles, and it can be explained by the thermal fluctuation of the Brownian motion as well as the imperfection within a single chain. For the ER nano-suspension, a single chain would play a similar role in a thick column for the ER micro-suspension. The plastic response has not yet been confirmed in our case, but the metastable configuration for the ER micro-suspension would be unstable for the ER nano-suspension because of the Brownian motion.

In Fig. 5, both G' and G'' at a given angular frequency increase with an increase in the strength of the electric field. The storage and loss moduli measured at an angular frequency of 1.9 rad·s^{-1} are plotted logarithmically in Fig. 7 against the strength of the electric field. The gap distance between the parallel plates was a narrower one at each electric field strength. In the figure, $G'(0)$ [or $G''(0)$] is the storage [or loss] modulus under no external electric fields, and the solid [or broken] arrow indicates the value. Clearly, G' is larger than G''. Above 2 kV·mm^{-1}, G' is proportional to E^2, and the E^2 dependence is quite consistent with the dipole–dipole interaction of dielectric particles.

However, G'' shows a slightly weaker dependence than E^2. If the microstructure is purely elastic, G'' should be zero. Therefore, the nano-suspension was rather viscoelastic even at 16 kV·mm^{-1}. On the other hand, G' [or G''] at 0.1 kV·mm^{-1} is almost the same as $G'(0)$ [or $G''(0)$]. Below 2 kV·mm^{-1}, G' is larger than the line showing the E^2 dependence. The upward deviation from the E^2 dependence would be caused by the particle–particle interaction without external electric fields. The dependence of G' (or G'') on E can be roughly divided into two regions, Region I below 2 kV·mm^{-1}, and Region II above 2 kV·mm^{-1}.

In the case of the ER micro-suspension with G' being strongly frequency-dependent, the upward (or no) deviation

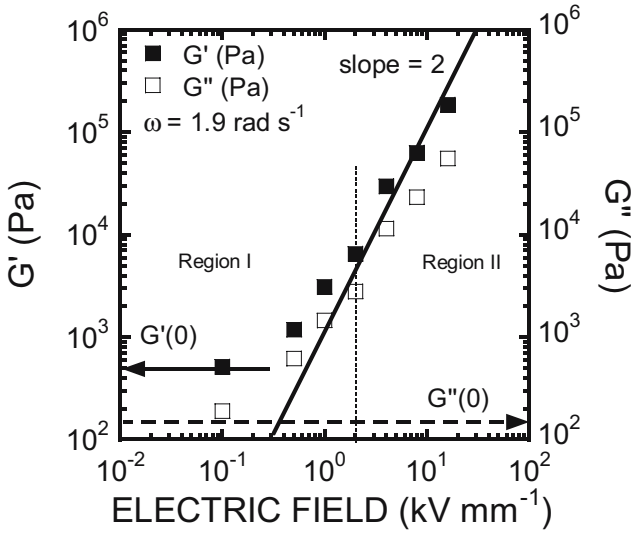

Fig. 7 The storage and loss moduli measured at 1.9 rad·s^{-1} plotted logarithmically against the strength of the electric field. The gap distance between the parallel plates was narrower at each electric field strength. In the figure, $G'(0)$ [or $G''(0)$] is the storage [or loss] modulus under no external electric fields, and the *solid* [or *broken*] *arrow* indicates the value

from the E^2 dependence could be found depending on ω. However, $G'(0)$ was not reported [15]. Therefore, a possible upward deviation is not related to the particle–particle interaction under no external electric fields. Unlike the micro-suspension, both the dynamic moduli were independent of ω for our nano-suspension even under no external electric fields. Still, the upward deviation from the E^2 dependence is clearly seen in Fig. 7.

In Fig. 8, G'' shown in Fig. 7 is logarithmically plotted against G'. In Region I, G'' is mostly proportional to G', while a weaker dependence of G'' than G' is found in Region II. The nano-suspension would essentially be isotropic under no external electric fields, and transient microstructures should be induced by the electric field in Region I. It can be thought that the nano-suspension was unstable, including some defects in Region I. In Region II, the anisotropic microstructure shown in Fig. 4 would be more stable and defect-free along the electric field.

Responses and relaxations of dynamic moduli induced by application and removal of the stepwise electric field

As discussed in Figs. 2 and 5, G' (or G'') is independent of ω. It is of interest that the nano-suspension is solid-like, having a possible isotropic microstructure under no external electric fields. The microstructure would be induced by a balance between an attractive particle–particle interaction under no external electric fields and thermal randomization by the Brownian motion. The initialization of the nano-suspension by steady shear before each dynamic measurement would also be an important factor in the present study.

Under the electric field, the nanoparticles are polarized and the dipole–dipole interaction is induced. Then, the chain-like microstructure is induced along the electric field. After removal of the electric field, the dipole–dipole interaction is also removed.

As a result, the response and relaxation of G' (or G'') would be rheologically observed. The relaxation of G' (or G'') would be controlled by a balance between an attractive interaction of particles confined in the chain-like microstructure after removal of the electric field and thermal randomization by the Brownian motion. In the present study, the responses and relaxations were measured with time for the dynamic moduli at a given ω induced by application and removal of the stepwise electric field.

Figure 9a and b shows the storage (a) and loss (b) moduli measured at a strain with γ_0 of 0.5% and ω of 3.14 rad·s^{-1} plotted logarithmically against time. The dc electric field was applied and removed stepwisely. Before and after the measurement of the first run, the nano-suspension was initialized by steady shear at 200 s^{-1} for 30 s, and kept in the quiescent state for 300 s. Following the initialization after the first run, the nano-suspension was measured under no external electric fields, which is denoted by each strength of the electric field for the first run. Under no electric fields, the second run was repeatedly measured following the initialization after the first run. Approximately 300 s after the second run, the third run was also measured without the initialization, followed by further measurement after the initialization.

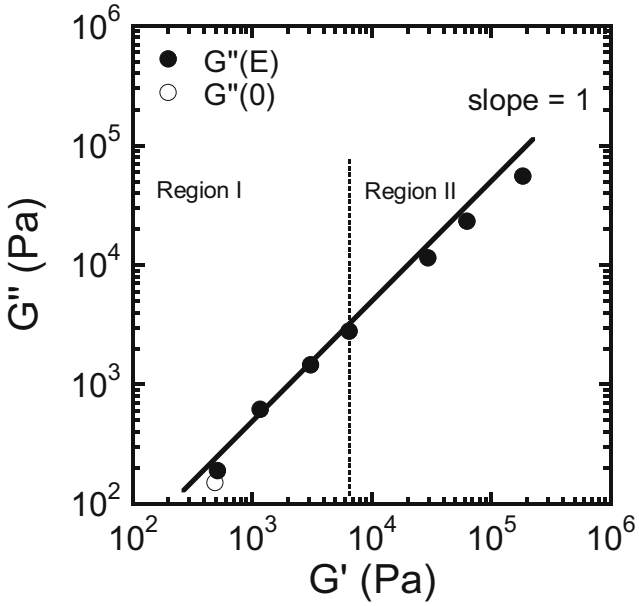

Fig. 8 The loss modulus shown in Fig. 7 plotted logarithmically against the storage modulus measured at 1.9 rad·s^{-1}. In the figure, $G''(0)$ is the loss modulus under no external electric fields, and $G''(E)$ is that under the dc electric field

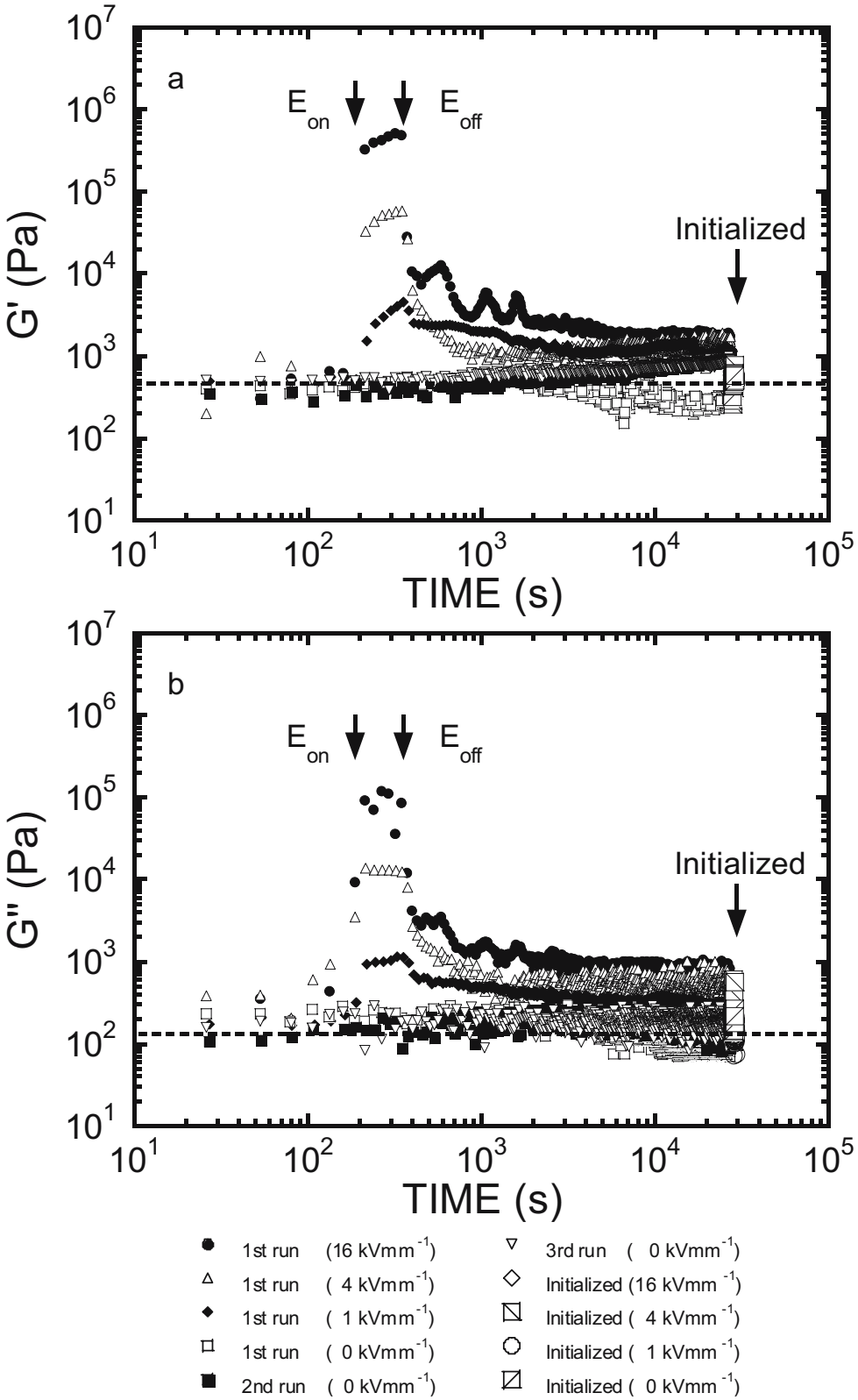

Fig. 9 The storage (**a**) and loss (**b**) moduli measured at a strain with γ_0 of 0.5% and ω of 3.14 rad·s^{-1} plotted logarithmically against time. The dc electric field was applied and removed stepwisely. Before and after the first run, the nano-suspension was initialized by steady shear at 200 s^{-1} for 30 s, and kept in the quiescent state for 300 s. The nano-suspension was then measured under no external electric fields, which is denoted by each electric field strength for the first run. Under no electric fields, the second run was repeatedly measured after initialization. Immediately after the second run, the third run was also measured without the initialization, followed by further measurement after the initialization

Under no electric fields, G' (or G'') in the first run mostly remains around the initial value shown in Fig. 9. However, G' (or G'') in the second and third runs after 10^3 s shows a different behavior from the first run behavior, although the difference in G'' is not pronounced. It is noted that even after initialization, G' in the second run gradually increases and reaches a saturated value after 10^4 s. Further, the initial value of G' in the third run without the

initialization is slightly smaller than the saturated value in the second run, and G' in the third run shows a similar increase. The saturated value of the third run is identical to that of the second run.

Immediately after the initialization, G' (or G'') mostly recovers around the initial value. Therefore, no remarkable increase or decrease in G' (or G'') is induced in the first run under no electric fields, and the history of the small oscillatory strain is negligible for a time scale of around 10^4 s. However, a slight increase in the saturated value can be induced in the second and third runs, suggesting that the history of the oscillatory strain was not completely initialized and a slightly more developed microstructure was induced under no electric fields by the competition among the attractive particle–particle interaction, the history of oscillatory strain, and thermal randomization by the Brownian motion.

On the other hand, G' (or G'') shown in Fig. 9 responds immediately to the application of the electric field. After the removal of the electric field, G' (or G'') immediately relaxes. After the fast relaxation, G' (or G'') also shows a much slower relaxation. (In the figure, the stress overshoot in response to the application of the electric field and dumping oscillation in relaxation especially after removal of the electric field of 16 kV·mm^{-1} are observed, which can be caused by the inertia of the upper plate of the rheometer.) The value of G' (or G'') for the last 10^4 s is mostly saturated. Similar to the results under no electric fields during the second and third runs, the saturated value is slightly larger than the initial value, although the saturated value of G'' shows slight differences.

It is noted that the saturated value of G' is quite consistent with that of the second and third runs under no electric fields. Furthermore, G' (or G'') mostly recovers around the initial value immediately after the initialization. (Results similar to the first run were observed in the second run after the initialization, followed by the application and removal of the electric field of 4 kV·mm^{-1}, except that the slow relaxation was much slower, and the saturated value of G' (or G'') was not found definitely).

The fast response to the applied electric field is essentially related to the formation of the chain-like microstructure induced by the competition among the attractive particle–particle interaction under no external electric fields, the (induced) dipole–dipole interaction, and thermal randomization by the Brownian motion. In the following discussion, the history of the oscillatory strain on a time scale of around 10^4 s is neglected, although it may be a factor after application and removal of the electric field. Essentially, no significant effect by the history of oscillatory strain would be induced without an attractive interaction of the particles.

The fast relaxation would be controlled by a balance between the attractive interaction of particles weakly aggregated near the surface within the chain-like microstructure after removal of the electric field and thermal randomization by the Brownian motion. It is noted that the nano-suspension also shows a slow relaxation on time scales much longer than 10^2 s after removal of the electric field. The contribution of the fast relaxation for the electric field corresponding to Region II, 4 and 16 kV·mm^{-1}, is much larger than the contribution corresponding to Region I, 1 kV·mm^{-1}.

The slow relaxation would be controlled by another balance between the attractive interaction of particles strongly aggregated and confined in the chain-like microstructure after removal of the electric field and thermal randomization by the Brownian motion. If the relaxation is controlled only by the Brownian motion, the time scale for the relaxation (τ_D) is roughly estimated by the one-dimensional diffusion of a primary particle to a distance [18].

$$\tau_D \sim 3\pi\eta_0 a_0 \langle x^2 \rangle / kT \tag{3}$$

where η_0 is the viscosity of the silicone oil of 5×10^{-2} Pa·s, a_0 is the radius of the primary particles of 7.5×10^{-9} m, $\langle x^2\rangle^{1/2}$ is the diffusion distance, k is Boltzmann constant, and T is the absolute temperature around 290 K. If $\langle x^2\rangle^{1/2}$ is roughly and overestimated around 1×10^{-5} m for a width of a single chain-like microstructure, τ_D is around 10^2 s. Typically, a_0 is chosen for a diffusion distance, $\langle x^2\rangle^{1/2}$. Then, τ_D is around 5×10^{-5} s.

The estimated time scales are much shorter than the time scales observed in the present study. For the relaxation of non-interacting particles in the chain-like microstructure, the relaxation is essentially controlled by the Brownian motion. The small oscillatory strain with ω of 3.14 rad·s^{-1} is negligible during the relaxation because τ_D, typically estimated around 5×10^{-5} s, is much shorter than the time scale of ω^{-1}. Furthermore, the linear responses were confirmed for γ_0 of 0.5% even under no electric fields. Therefore, not only the Brownian motion, but also the attractive interaction of particles strongly aggregated and confined in the chain-like microstructure after removal of the electric field, play a significant role in the slow relaxations of the dynamic moduli.

Finally, both linear dynamic moduli of the nano-suspension were mostly independent of ω, and G'' was smaller than G' in the presence and absence of the electric field, as shown in Figs. 2 and 5. As discussed earlier, a possible isotropic microstructure, such as a three-dimensional network of nanoparticles, would be developed under no electric fields, while a fine chain-like microstructure of nanoparticles was observed under the dc electric field. Both

microstructures of nanoparticles would be relatively unstable, including some defects. Therefore, the energy dissipation can be caused by the rearrangement of the nanoparticles within each microstructure. The oscillatory strain would be a factor for the rearrangement. Furthermore, the results of the relaxations after removal of the electric field show that the Brownian motion and attractive interactions of nanoparticles are essential factors for the fast and slow relaxations. The rearrangement can also be induced by thermal fluctuation of the Brownian motion with attractive interactions of the nanoparticles.

Conclusions

In the present study, the linear viscoelastic properties of a suspension composed of TiO_2 nanoparticles were measured under no external electric fields and the dc electric field with narrow gap distances between the electrodes. No remarkable wall slip was observed at the interface between the parallel plates and the nano-suspension. The yielding behavior under no external electric fields was also reported. Furthermore, a fine chain-like microstructure was optically observed within a narrow gap between the electrodes under the dc electric field in the quiescent state, and the hierarchical structure of the nanoparticles was also found within a single chain. The chain-like microstructure was responsible for the ER effect of the nano-suspension. The nano-suspension confined to a narrow gap between the parallel plates was rather viscoelastic at the highest electric field strength in the present study.

The significant role of not only the Brownian motion, but also the attractive interaction of particles strongly aggregated and confined in the chain-like microstructure after removal of the electric field, was discussed during the slow relaxations of the dynamic moduli. The energy dissipation in the nano-suspension was also discussed in terms of the rearrangement of nanoparticles within the microstructures in the presence and absence of the electric field. It was pointed out that the linear viscoelasticity was an appropriate measure of the microstructure before yielding.

References

1. Winslow WM (1949) J Appl Phys 20:1137
2. Block H, Kelly JP, Qin A, Watson T (1990) Langmuir 6:6
3. Filisko FE, Radzilowski LH (1990) J Rheol 34:539
4. Conrad H, Sprecher AF, Choi Y, Chen Y (1991) J Rheol 35:1393
5. Otsubo Y, Edamura K (1995) J Colloid Interface Sci 172:530
6. Tanaka K, Wakayasu T, Kubono A, Akiyama R (2004) Sens Actuators A 112:376
7. Kraynic AM (1990) In: Carlson JD, Sprecher AF, Conrad H (eds) Proceedings of the 2nd International Conference on ER Fluids. Technomic Publishing, Lancaster, pp. 445
8. Barnes HA, Walters K (1985) Rheol Acta 24:323
9. Hartnett JP, Hu RYZ (1989) J Rheol 33:671
10. Yoshimura A, Prud'homme RK (1987) J Rheol 31:699
11. Tanaka K, Ichizawa K, Akiyama R, Kubono A (2001) Nihon Reoroji Gakkaishi (J Soc Rheol, Jpn) 29:105
12. Onogi S, Masuda T, Matsumoto T (1970) Trans Soc Rheol 14:275
13. Tanaka K, Akiyama R, Takano M, Kutsumizu S, Yamaguchi T (2004) Trans Mater Res Soc Jpn 29:815
14. Tanaka K, Fujioka Y, Kubono A, Akiyama R (2006) Colloid Polym Sci 284:562
15. Parthasarathy M, Ahn KH, Belongia BM, Klingenberg DJ (1994) Int J Mod Phys B 8:2789
16. Otsubo Y, Sekine M, Katayama S (1992) J Rheol 36:479
17. Tao R, Sun JM (1991) Phys Rev Lett 67:398
18. Tao R, Xu X (2006) Energy Fuels 20:2046